

Development and demonstration of a higher temperature PEM fuel cell stack

Leonard J. Bonville^a, H. Russell Kunz^a, Ying Song^{b,*}, Anthony Mientek^b,
Minkmas Williams^b, Albert Ching^b, James M. Fenton^{a,b}

^a *Ionomem Corporation, University of Connecticut, Environmental Research Institute, 270 Middle Turnpike Unit 5210, Storrs CT 06269, USA*

^b *University of Connecticut, Department of Chemical Engineering, 191 Auditorium Road, Storrs CT 06269, USA*

Received 15 November 2004; received in revised form 19 December 2004; accepted 19 December 2004

Available online 16 March 2005

Abstract

Research and development was conducted on a proton exchange membrane (PEM) fuel cell stack to demonstrate the capabilities of Ionomem Corporation's composite membrane to operate at 120 °C and ambient pressure for on-site electrical power generation with useful waste heat. The membrane was a composite of polytetrafluoroethylene (PTFE), Nafion[®], and phosphotungstic acid. Studies were first performed on the membrane, cathode catalyst layer, and gas diffusion layer to improve performance in 25 cm², subscale cells. This technology was then scaled-up to a commercial 300 cm² size and evaluated in multi-cell stacks. The resulting stack obtained a performance near that of the subscale cells, 0.60 V at 400 mA cm⁻² at near 120 °C and ambient pressure with hydrogen and air reactants containing water at 35% relative humidity. The water used for cooling the stack resulted in available waste heat at 116 °C. The performance of the stack was verified. This was the first successful test of a higher-temperature, PEM, fuel-cell stack that did not use phosphoric acid electrolyte.

© 2005 Elsevier B.V. All rights reserved.

Keywords: PEM fuel cell; Stack; Performance; High temperature

1. Introduction

One of the most promising types of fuel cells, the proton exchange membrane (PEM) fuel cell, is currently being aggressively researched and developed for use in on-site electrical power generation for the replacement of the internal combustion engine in vehicle applications and for portable power. These cells allow better vehicular fuel economy because they are inherently more efficient than internal combustion engines. They also meet more stringent emissions standards because they produce far fewer pollutants than internal combustion engines. Despite these advantages, significant obstacles to commercialization remain in the areas of cost, durability, heat and water management, freeze protec-

tion, and tolerance to poisons (such as carbon monoxide) in the fuel.

The University of Connecticut (UConn) has developed an innovative higher temperature proton exchange membrane electrode assembly (HTMEA) that provides both excellent ionic conductivity within the membrane and improved electrode structures for use in an under-saturated environment [1]. This environment has a severe adverse effect on present PEM fuel cells because loss of water from the ionomeric electrolyte results in a greatly reduced performance. Fig. 1 shows the strong dependency of commercial Nafion[®] 112 perfluorosulfonic acid membrane and UConn in-house membrane on the relative humidity in the gas contacting the membrane at 120 °C.

At UConn, solid proton conductors, such as phosphotungstic acid or zirconium hydrogen phosphate, are incorporated with Nafion[®] in the ionomeric electrolyte

* Corresponding author. Tel.: +1 860 486 6675; fax: +1 860 486 5488.
E-mail address: yingsong_2003@yahoo.com (Y. Song).

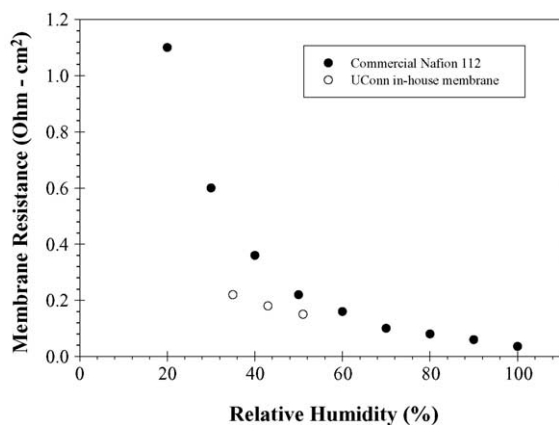


Fig. 1. Resistance of commercial Nafion[®] 112 membrane and UConn In-house membrane as a function of relative humidity at 120 °C.

to provide more water-independent ionic conduction and achieve improved performance at higher temperatures (120 °C) at atmospheric pressure. This higher-temperature operation increases power density, specific power, and durability through system and component simplification. Higher temperature enhances carbon monoxide tolerance and eliminates the need for a selective oxidizer in the fuel stream. Enhanced heat transfer due to increased temperature differences decreases mass and volume required for heat rejection. Higher-quality waste heat increases system efficiency through cogeneration, and simplifies water management. The waste heat can be used to produce steam if a hydrocarbon fuel is used to produce hydrogen using a steam-reform reaction. The under-saturated operating environment alleviates mechanical stress imparted by water expansion upon freezing and facilitates rapid start-up in freezing conditions because melting ice becomes unnecessary. Enhanced freeze tolerance and reduced system complexity makes the system more durable. Cogeneration of useful waste-heat makes the system more cost-effective and efficient. The fact that the cell operates at near atmospheric pressure means that a compressor that would reduce system efficiency is not needed.

The objective of this program was to advance the higher temperature membrane and electrode assembly technology from the laboratory scale to full-scale demonstration in a multi-cell stack. Several features of higher-temperature PEM fuel cell stack technology were demonstrated, including cell component scale-up, cell performance improvement, and post-test analysis and evaluation.

2. Experimental program

Development activities were performed on all of the components of the fuel cell stack—the membrane, the catalyst layers, the gas diffusion layers, and the complete stack assembly.

2.1. Membrane

The membrane used in this program had a tri-layer structure. The central region consisted of a composite electrolyte of Nafion[®] and solid phosphotungstic acid (PTA) impregnated into a highly porous sheet of polytetrafluoroethylene (PTFE). On each surface of this central region, a coating of the Nafion and PTA were applied. This tri-layer arrangement was used to provide better contact between the catalyst layers that were applied to both surfaces of the membrane. The PTFE core was used to add strength to the membrane and allow the membrane thickness to be reduced to about 25 μm to result in lower cell resistance. The resistance of Nafion-based membranes increases as the water content is reduced. Since this membrane is thin, the water produced at the cell cathode during operation can permeate through the membrane and improve its conductivity.

Prior to the start of this demonstrator program, good membrane conductivity had been demonstrated at UConn in PEMFCs of 5 and 25 cm² active area. This program required that this technology be scaled up to 300 cm² area.

The Nafion[®], PTFE, phosphotungstic acid (NTPA) membranes in this program were all produced by hand using the approach shown in Fig. 2. A porous PTFE sheet was mounted in a hoop, and the composite electrolyte applied. After drying, additional composite electrolyte was applied to each surface and the tri-layer membrane dried.

2.2. Catalyst layers

Concurrent with the membrane scale-up, activities were undertaken for significant performance improvement based upon optimization of the membrane-electrode-assembly (MEA) electrode structure for the under-saturated, high-temperature, PEMFC environment. Improved quality and process control techniques were also implemented.

During this program, 47 individual 25 cm² cells were fabricated and tested to identify manufacturing steps and proce-



Fig. 2. Fabrication of a composite membrane for the fuel cell.

dures that needed improvement for scale-up to full-size cells and to demonstrate reproducible performance with the baseline processes. Specific issues addressed in this testing were:

- catalyst selection and qualification;
- catalyst ink formulation;
- performance reproducibility;
- verification of scale-up process for MEAs.

The first step of scale-up from the research laboratory scale (5 cm² cell active area) to a useable commercial scale was a series of three tests at 25 cm². The analysis of these cells tested showed that they reproduced the performance previously seen with the 5 cm² laboratory cells. The performances were 0.462, 0.468 and 0.436 mV at 400 mA cm⁻² at 120 °C on H₂/air. All of these cells were an initial baseline design using Pt/Ru black with Pt/Ru on carbon sublayer as the anode catalyst and Pt black with a Pt/carbon sublayer at the cathode. These catalysts were applied to the membranes using a spray technique. The blacks of about 0.4 mg precious metal cm⁻² were first applied to the membrane and the supported catalyst applied over that layer. The supported catalyst loading was about 10% of the black loading.

Much of the work of performance improvement involved the evaluation of alternative cathode catalysts. The evaluation of these catalysts involved the optimization of the cathode structure. The results of this study are being published elsewhere [2].

Four cathode catalysts were studied: platinum black (Alfa Aesar, Ward Hill, MA), 40 wt.% Pt/C (Alfa Aesar, Ward Hill, MA), 15 wt.% Pt/C and 47 wt.% Pt/C (Tanaka Kikinzo Kogyo, Tokyo Japan). The catalysts were thoroughly mixed with Nafion[®] solution by ultrasonic stirring before they were applied to the membrane by spraying. Nafion[®] content for four cathode catalysts ranged from 10 to 40 wt.%. Cathode platinum loading was studied with the 15 and 46.5 wt.% Pt/C catalyst layers. The membrane electrode assemblies were prepared using a method developed at Ionomem Corporation using NTPA membranes manufactured in-house. The performances of cells using these four catalysts at 120 °C, atmospheric pressure, and 35% relative humidity hydrogen and oxygen reactants are shown in Fig. 3. The performance of the platinum black catalyst was found to be greatly improved by the use of a pore-former to enhance catalyst effectiveness and oxygen diffusion into the catalyst layer [3].

In addition to the determination of cell performance, several characteristics of the catalysts were measured in this study. Some of these are presented in Fig. 4. The total surface area, pore volume, and pore size were determined using the BET nitrogen adsorption technique, and the platinum surface area was measured by electrochemical hydrogen adsorption in an actual fuel cell. The 46.5 wt.% catalyst resulted in the best performance because of its high catalytic activity associated with the high platinum surface area. This high surface area is related to the high surface area of the carbon support used for the platinum. The high platinum concentration on this catalyst resulted in a thin catalyst layer that

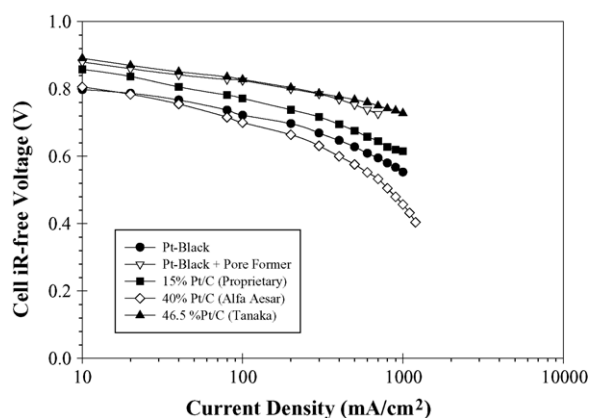


Fig. 3. Cell performance using various cathode catalysts (H₂/O₂, 1 atm, 120 °C, 35% relative humidity).

is beneficial from an oxygen diffusion and ionic conduction standpoint.

2.3. Gas diffusion layers

Various commercial gas diffusion layers were evaluated in the 5 and 25 cm² cells. Performance diagnostics done on the cells indicated that the gas diffusion layers were contributing to a poor cell performance. Therefore, a new gas diffusion layer configuration was developed that improved the performance. That layer consisted of a Toray carbon paper layer with a Vulcan XC-72/Teflon[®] layer screen-printed onto one surface. The properties and characterization of that gas diffusion layer has been published elsewhere [4].

A comparison of the cell performance obtained with that gas diffusion layer and commercial layers is shown in Fig. 5. The commercial layers consisted of four types manufactured by E-TEK (E-TEK Inc., Somerset, NJ) and one fabricated by SGL (SGL Carbon Group, Short Hills, NJ). These performance curves were obtained in 5 cm² cells using hydrogen and air reactants at 120 °C cell temperature with both inlet reactants saturated at 35% relative humidity (90 °C dew point). The air utilization was 33% and the hydrogen utilization 25%.

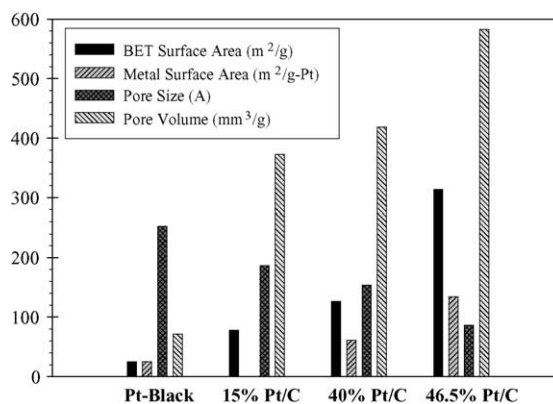


Fig. 4. Four cathode catalyst characteristics [2].

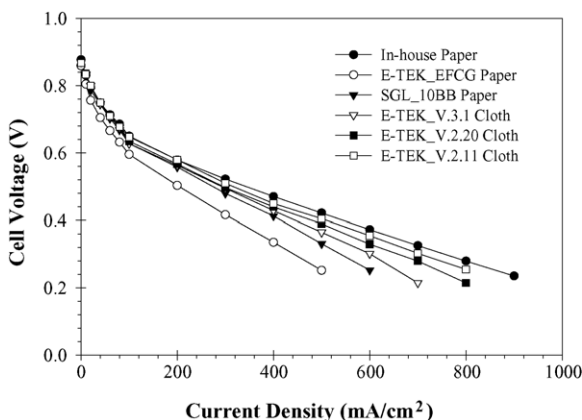


Fig. 5. Performance comparison using various gas diffusion layers (H_2/Air , 1 atm, 120°C , 35% relative humidity) [4].

In preparing these membrane electrode assemblies, cathode and anode catalyst inks were sprayed directly onto each side of an Ionomem higher-temperature Nafion[®]-PTFE-phosphotungstic acid composite membrane ($25 \pm 2 \mu\text{m}$ in thickness). The catalyst-coated membrane was then sandwiched between two gas diffusion layers to obtain a 5 cm^2 MEA for single-cell polarization measurement. The cathode catalyst was 40 wt.% Pt/C (Alfa Aesar, Ward Hill, MA) and the anode catalyst was 40 wt.% Pt–Ru/C with 1:1 atomic ratio (E-TEK Inc., Somerset, NJ). Nafion[®] loading in the catalyst ink was 25 wt.% for both the cathode and the anode. Cathode and anode loading of precious metals was $0.45 \pm 0.05 \text{ mg cm}^{-2}$ each.

The performances of two 25 cm^2 cells using the Tanaka catalyst and new gas diffusion layer are shown in Fig. 6. This figure shows the performance of the two cells at both 80 and 120°C using hydrogen and air as the reactants. For the 80°C condition, the reactants were saturated with water vapor. For the 120°C case, the conditions were similar to the 5 cm^2 cells described above. The performances of the two cells at 120°C are nearly identical and are about 0.6 V

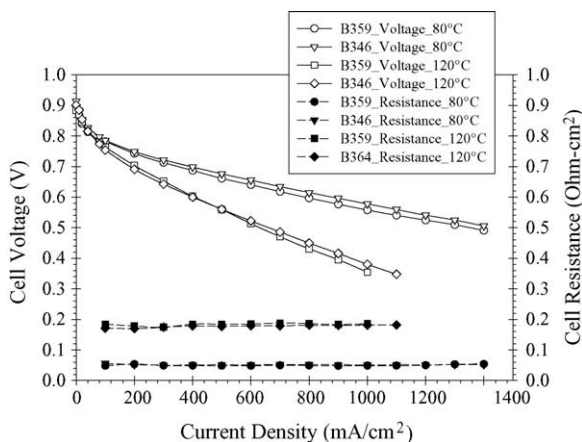


Fig. 6. Comparison of performance of two cells at both 80 and 120°C (H_2/Air , 1 atm).

at 400 mA cm^{-2} current density. The cell resistances at the two temperatures are also plotted in the figure and are about $0.05 \Omega \text{ cm}^2$ at 80°C and $0.18 \Omega \text{ cm}^2$ at 120°C .

Numerous cells were assembled and tested to obtain the data for establishing the baseline catalyst ink formulation and catalyst application procedures. These cells incorporated membranes and gas diffusion layers cut from full-scale parts fabricated according to the scale-up procedures.

2.4. Stack configuration

Using the components evolved for performance improvement, a stack was designed to demonstrate that performance in a realistic stack size. The stack design selected had the following configuration:

- four cells;
- 300 cm^2 cell active area;
- commercial unsupported Pt/Ru anode catalyst;
- commercial Pt on carbon cathode catalyst;
- unitized membrane-electrode-assemblies with integral seals;
- sweep flow field for fuel (hydrogen);
- interdigitated flow field for air, cross-flow with fuel;
- fine channel water-cooling between each cell;
- external air manifold;
- internal fuel (hydrogen) manifold;
- plated machined end plates.

The design of the MEA is shown in Fig. 7. Several stacks were tested prior to the final 300 cm^2 demonstrator stack. In order to clearly demonstrate the quality of the waste heat provided by the stack, a cooling cart, shown in Fig. 8, was fabricated to simulate the device, such as a home, that uses that heat.

After assembly, the demonstrator stack (B27) had a pretest checkout prior to performance testing. This checkout consisted of the determination of internal leakage, external leakage, and the presence of any electronic short circuits between components. These results were found to be acceptable and the stack was put on test. The performance data are shown in Fig. 9.

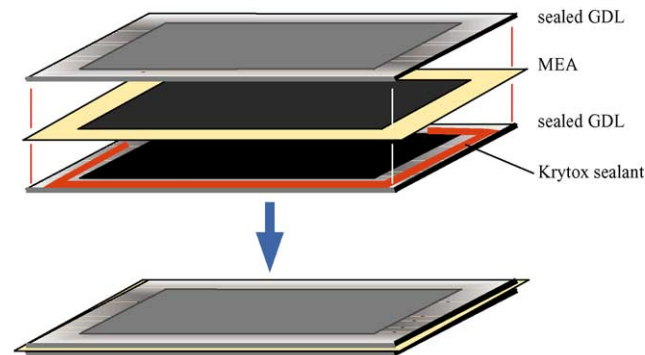


Fig. 7. Component lamination to produce the unitized MEA.

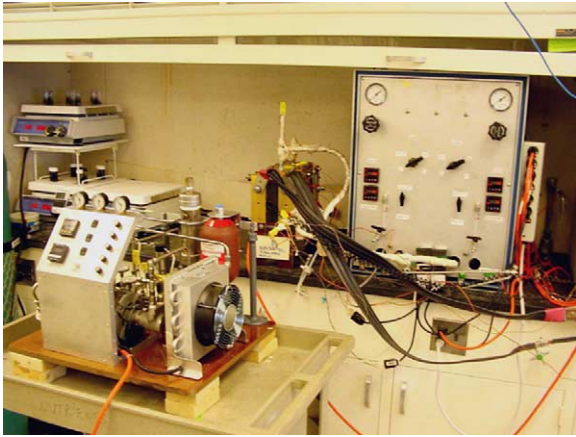


Fig. 8. Cooling cart and demonstrator stack at test.

This figure shows the performance of the stack at 110–116 °C and ambient pressure using both hydrogen/oxygen and hydrogen/air as the reactants saturated at 90 °C. This was done to help diagnose the performance characteristics. The performance on air was about 2.34 V at 400 mA cm⁻², resulting in an average voltage of each cell being 0.59 V, about the same as seen in the 25 cm² single cell testing mentioned above. The resistance of the stack measured using a current-interrupt technique is also shown. That resistance is 0.65 Ω cm², resulting in an average cell resistance of 0.16 Ω cm², somewhat better than the 0.18 Ω cm² measured in the smaller cells. Slight differences would be expected because the stack was operated at a lower average temperature (110–116 °C) than that of the subscale cells. Those cells were electrically heated to a uniform temperature while a temperature gradient occurred across the stack because it was water-cooled. The cooling water inlet temperature was 110 to 112 °C and the outlet temperature 116 °C.

The demonstrator stack was further tested at a lower temperature of 100 °C since interest had been expressed in this operating temperature for a near-term application. These data are shown in Fig. 10.

At the lower operating temperature, the stack performance increased to 2.57 V at 400 mA cm⁻² (0.64 V per cell). This

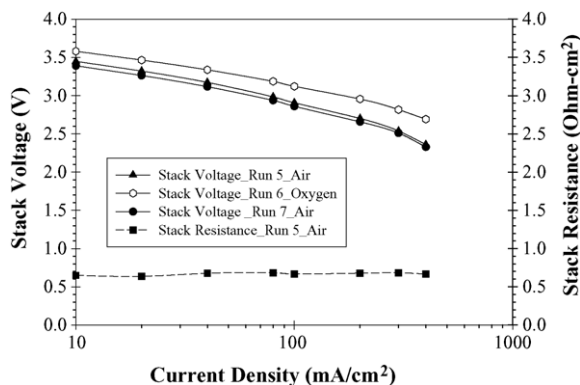


Fig. 9. Performance of demonstrator 4-cell stack, day 2, at 110–116 °C.

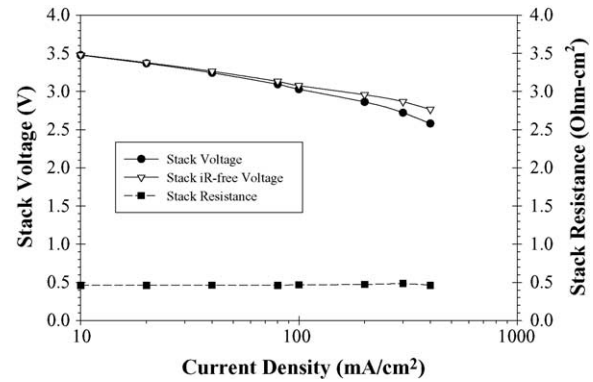


Fig. 10. Performance of demonstrator 4-cell stack, day 2, air, at 100 °C.

level is very acceptable for near term applications. The cell resistance decreased to 0.11 Ω cm² because the relative humidity of the reactants increased as the cell temperature was reduced.

The overall stack voltage at 400 mA cm⁻² and the higher temperature remained at 2.46 V during day-3 testing, as shown in Fig. 11. The cell resistance also remained good at 0.14 Ω cm².

3. Discussion

The present stack performance at 80 °C was compared with that of three commercial manufacturers at the lower temperatures, 65–70 °C, that they typically use. Other conditions are atmospheric pressure using hydrogen and air as the reactants and similar catalyst loadings [5–7]. This comparison is shown in Fig. 12. The present stack can be seen to provide performance near that of these manufacturers at lower temperatures. At these conditions, the higher published data indicate that a current density of 600–700 mA cm⁻² can be obtained at 0.7 V.

At the higher temperature, as shown in Fig. 12, the present stack resulted in a cell current density of about 200 mA cm⁻² at the same 0.7 V. This means that the stack would have to be larger to result in the same cell voltage (efficiency) as at the

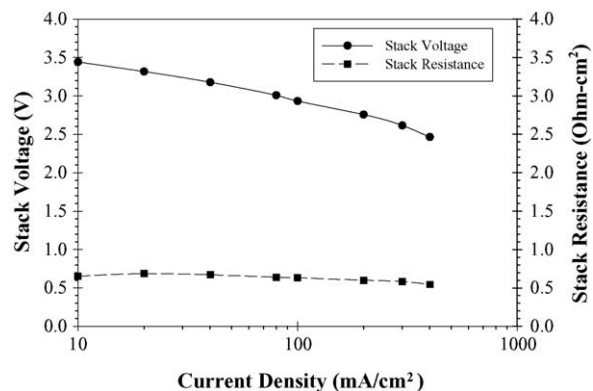


Fig. 11. Performance of demonstrator stack, air, day 3, at 110 °C.

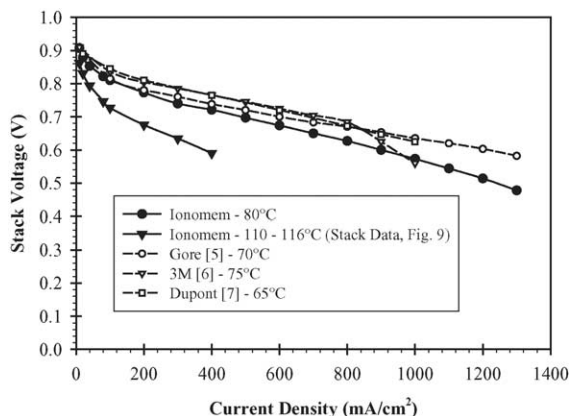


Fig. 12. Comparison of PEM cell performance of various manufacturer [5–7].

higher temperature. However, that stack would integrate into a much more efficient system with respect to waste heat and carbon monoxide tolerance as described previously. This performance at near 120 °C is above that which can be obtained using hydrogen and air with polybenzimidazole/phosphoric acid electrolyte at higher temperatures such as 160 °C.

To test the off-design capability the cell was allowable to dry out by operating it with very low humidification. When the cell dried out, the performance was drastically reduced. Subsequently, the cell was wetted up and the performance returned to previous levels. The ability to achieve a performance recovery is shown in Fig. 13. There is almost no effect of a dry-out condition on the subsequent cell performance and resistance. The ability of MEA to recover performance from a dry-out condition is very critical to the reliability in commercial applications.

With respect to the endurance capability of the demonstrator stack, it was never endurance tested in the present program due to the facility limitation in the laboratory. However, subscale 25 cm² cells were subjected to short-term stability tests. The results of one of those tests are shown in Fig. 14. This test showed that the cell performance and resistance at 400 mA cm⁻² on hydrogen/air reactants were stable in the test period of 90 h at 105 °C.

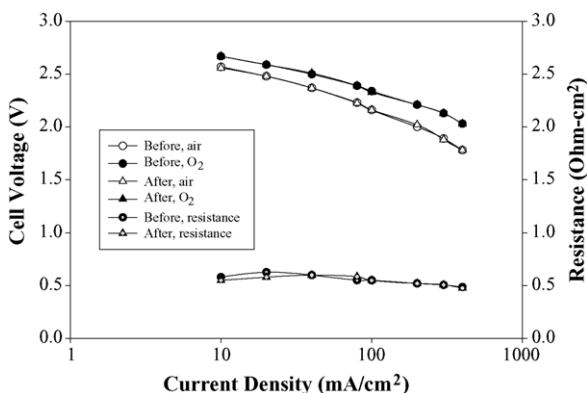


Fig. 13. Recovery test from dry-out condition.

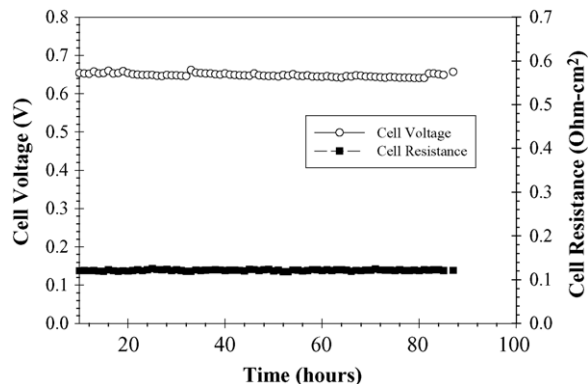


Fig. 14. Short-term stability test voltage on a subscale cell at 400 mA cm⁻² (H₂/Air, 1 atm, 105 °C, 58% relative humidity).

4. Conclusions

This research and development program resulted in a full-scale stack that successfully demonstrated the Ionomem higher temperature membrane. This stack operated at about 120 °C with near-ambient pressure reactants saturated at 90 °C and provided a cell voltage in excess of 0.5 V at a current density of 400 mA cm⁻² using hydrogen and air reactants. The stack incorporated conventional bipolar plates and provided thermal energy to water coolant fluid in a separate cooling cart. In this demonstration program, Ionomem implemented 300 cm² membrane electrode assembly (MEA) batch-process fabrication that can be scaled to produce larger stacks. Endurance verification of this design is still required.

Acknowledgements

Ionomem acknowledges the support provided by this Connecticut Light & Power Company (CL&P) research and development program and the University of Connecticut in the performance of this program.

References

- [1] J.M. Fenton, H.R. Kunz, M.B. Cutlip, J.-C. Lin, US Patent 6,465,136 (2002).
- [2] Y. Song, L. Bonville, H.R. Kunz, J. Fenton, Power sources for transportation applications, in: Proceeding Volume from The Electrochemical Society 206th Meeting, Orlando, FL, USA, Fall 2003, in press.
- [3] Y. Song, Y. Wei, H. Xu, M. Williams, Y. Liu, L.J. Bonville, H.R. Kunz, J.M. Fenton, J. Power Sources 141 (2005) 250–257.
- [4] M.V. Williams, E.K. Begg, L.J. Bonville, H.R. Kunz, J.M. Fenton, J. Electrochem. Soc. 151 (2004) A1173–A1180.
- [5] T. Gu, W.-K. Lee, J.W. Van Zee, M. Murthy, The Electrochemical Society 202nd Meeting, Meeting, Salt Lake City, UT, US Fall 2002 (abstract #830).
- [6] Fuel Cells for Transportation 2001. Annual Progress Report, US Department of Energy, Office of Advanced Automotive Technologies, Approved by Steven Chalk, 2001, pp. 119.
- [7] High Volume, low cost manufacturing process for Nafion[®] membranes, In: D.E. Curtin, M.A. Watkins (Eds.), Proceedings of the 2002 Fuel Cell Seminar Abstracts, 2002, p. 834.